Available online at www.sciencedirect.com
ScienceDirect
International Journal of Pharmaceutics 339 (2007) 33–38
INTERNATIONAL JOURNAL OF PHARMACEUTICS
www.elsevier.com/locate/ijpharm

Levofloxacin implants with predefined microstructure fabricated by three-dimensional printing technique

Weidong Huang [a], Qixin Zheng [b], Wangqiang Sun [a], Huibi Xu [c], Xiangliang Yang [a,*]

[a] *Institue of Materia Medica, Huazhong University of Science and Technology, Wuhan 430074, China*
[b] *Department of Orthopaedics, Union Hospital, Tongji Medical College, Huazhong University of Science and Technology, Wuhan 430022, China*
[c] *Department of Chemistry, Huazhong University of Science and Technology, Wuhan 430074, China*

Received 23 October 2006; received in revised form 11 February 2007; accepted 14 February 2007
Available online 23 February 2007

Abstract

A novel three-dimensional (3D) printing technique was utilized in the preparation of drug implants that can be designed to have complex drug release profiles. The method we describe is based on a lactic acid polymer matrix with a predefined microstructure that is amenable to rapid prototyping and fabrication. We describe how the process parameters, especially selection of the binder, were optimized. Implants containing levofloxacin (LVFX) with predefined microstructures using an optimized binder solution of ethanol and acetone (20:80, v/v) were prepared by a 3D printing process that achieved a bi-modal profile displaying both pulsatile and steady state LVFX release from a single implant. The pulse release appeared from day 5 to 25, followed by a steady state phase of 25 days. The next pulse release phase then began at the 50th day and ended at the 80th day. To evaluate the drug implants structurally and analytically, the microscopic morphologies and the in vitro release profiles of the implants fabricated by both the 3D printing technique and the conventional lost mold technique were assessed using environmental scanning electron microscopy (ESEM) and UV absorbance spectrophotometry. The results demonstrate that the 3D printing technology can be used to fabricate drug implants with sophisticated micro- and macro-architecture in a single device that may be rapidly prototyped and fabricated. We conclude that drug implants with predefined microstructure fabricated by 3D printing techniques can have clear advantages compared to implants fabricated by conventional compressing methods.

Keywords: Drug implant; Three-dimensional (3D) printing; Conventional compression mold; Drug release in vitro; Levofloxacin (LVFX)

1. Introduction

While the systemic route of drug administration is the mainstay of pharmacotherapy, it often suffers from limitations due to dose-limited efficacy or safety (Alekha and Greggrey, 1998; Achim, 1997). Drug implants are an alternative method of delivering drugs locally and can have significant advantages over systemic delivery for certain indications. Implants in or near the diseased organ that contain active drug within a sustained-release delivery matrix provide the benefits of relatively high therapeutic efficacy and low systemic toxicity. For example, retinal diseases are difficult to treat with systemically administered drugs because of the blood-retinal barrier, as well as due to systemic toxicity.

Drug implants are often manufactured by the freeform fabrication of a homogeneous mixture of the powder form of the active ingredient together with its excipients (Gabriel et al., 2002; Zheng et al., 2002; Zhou et al., 1998; Soriano and Evora, 2000; Castro et al., 2003). While these methods have merits, there can suffer from a lack of control over the structure and internal architecture of the implants, which can limit their effectiveness. The three-dimensional (3D) printing technique represents one of several improved technologies used more recently to produce drug implants (Sarah and Tejal, 2003; Wu et al., 1996). The 3D printing process is a type of solid, freeform fabrication technique first developed at MIT (Wu et al., 1996; Jill et al., 2002). The 3D printing process works in a manner very similar to an "ink jet" printer to create a precise, three-

* Corresponding author. Tel.: +86 27 8720 2711.
E-mail address: yangxl@mail.hust.edu.cn (X. Yang).

0378-5173/$ – see front matter © 2007 Published by Elsevier B.V.
doi:10.1016/j.ijpharm.2007.02.021

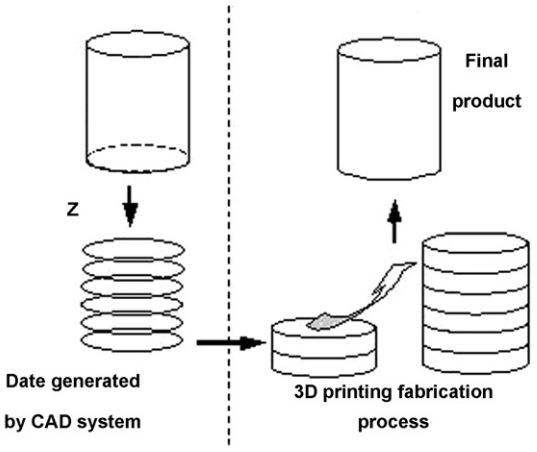

Fig. 1. The schematic illustration of the principle of the 3D printing.

dimensional product composed of a series of two-dimensional layers. A principle of the technique is presented in Fig. 1.

The essential elements of the printing device are a *z*-piston as a building box, an *x*–*y* plotter for moving the printing device, the spreading unit, and several electronic control devices. Unlike other conventional pharmaceutical processing technologies, 3D printing technology enables the design and fabrication of implants with novel and precisely defined, micro- and macro-architecture. The implants can be designed to have uniform drug distribution in the matrix form, display well-controlled dosing and have complex drug release profiles.

There have been several reports on the use of 3D printing methodologies in medical applications. Most of these have focused on the engineering aspects of fabricating scaffolds for tissue and organ replacements. For example, Kim et al. (1998) employed 3D printing with particulate leaching technique for creating porous scaffolds. The work of Park et al. (1998), Zeltinger et al. (2001) and Lam et al. (2002) deal mainly with 3D printing methods used for the fabrication of scaffolds made up of different polymer materials. Generally, there are few published studies on the application of 3D printing techniques to fabricate drug implants. The first report of using 3D printing process to fabricate drug delivery devices was by Wu et al. (1996), who showed it was possible to construct devices with complex microstructure, rather than just complex macro-shapes. However, their study used dyes as model drugs to demonstrate proof of concept for 3D printing in fabricating drug delivery devices. Katsta et al. (2000) and Rowe et al. (2000) reported that oral dosage forms of standard pharmaceuticals could be formulated with the aid of 3D printing methods.

In 3D printing methods, several parameters may be controlled to optimize the drug delivery properties of the implant. The layer thickness and spacing between printed lines are optimized to provide adhesion between lines and layers. Flow rate of the liquid binder and fast axis speed determine the quantity of binder deposited per unit line length. These operating parameters for fabricating implants were optimized in our previous study (Huang et al., 2005).

In this report, we describe the properties of implants fabricated by a 3D printing technique compared with a conventional compression method for fabricating implants for the controlled delivery of Levofloxacin (LVFX), a broad-spectrum fluoroquinolone antibiotic against gram-positive, gram-negative and atypical bacteria. A powder of biocompatible poly-L-lactide (PLA), a polymer of lactic acid, was developed to compare the 3D printing and conventional compression methods. Selection of the binder in the 3D printing process was optimized for manufacturing implant prototypes and with predefined microstructure, which we then fabricated and tested. The morphology of the implants manufactured by both processes was characterized and the release profiles of LVFX in vitro were studied.

2. Materials and methods

2.1. Materials

Poly (L-lactic acid) (L-PLA), M_w = 100 kDa, was a gift from Dikang Biomedical Co., Ltd. (Chengdu, China). Levofloxacin (LVFX) powder was obtained from Daiichi Pharmaceutical (Beijing) Co., Ltd. All other chemicals were analytical grade or better and readily available commercially.

Polymer L-PLA powders were milled, vacuum-dried and hand-sieved with stainless steel sieves at 150 μm before fabrication.

2.2. Implants design

Three cylindrical implants were designed as illustrated in Fig. 2 I–III. The names and dimensions of the designs are summarized in Table 1. L-PLA was chosen as the main

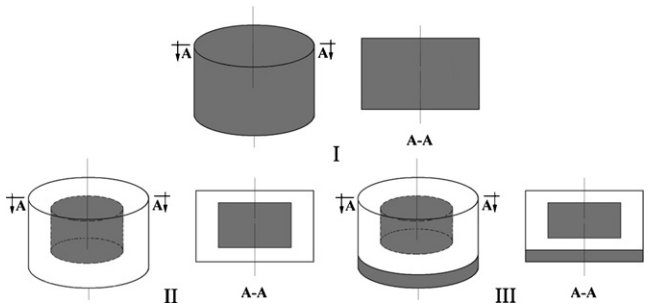

Fig. 2. The schematic illustration of the LVFX implant designs.

Table 1
Comparison of LVFX implants designs

	I	II	III
Implant design	Matrix structure	Capsule structure	Double-layer with a reservoir-like structure
Drug distribution	Homogeneous	Homogeneous in core portion	Homogeneous in lower and upper portion

matrix material because of its well-established biocompatibility, biodegradability, and FDA approval as biomaterial for clinical use.

The implant in Fig. 2 I was a single matrix structure with LVFX homogeneously distributed in L-PLA matrix. For comparison, we fabricated implant I in Fig. 2 using both the conventional compressing process and 3D printing technology. Implants with more intricate architectures were also designed by 3D printing technique, as shown in Fig. 2 II–III. Implant II has a capsule structure, with its core containing LVFX distributed in the matrix and surrounded by the L-PLA matrix. The implant III prototype consists of a complex structure: the upper region was a reservoir-like system, in which the homogeneous mixture of LVFX and L-PLA was encapsulated, while the lower region was a L-PLA matrix system homogeneously loaded with LVFX.

2.3. Fabrication of implants

2.3.1. Three-dimensional printing process

A 3D printing test setup was used for process evaluations. The machine was designed and built by Fochif Mechatronics Technology Co. Ltd. (Shanghai, China). We used 3D inkjet printing to create a solid object by printing a binder onto selected areas of sequentially deposited layers of powder or particulates in the following sequence:

1. Align the first desired powder cylinder with the rolling delivery system.
2. Increase the movable position piston upwards to deliver an incremental amount of powder.
3. Activate the roller to move powder to the receiving platform.
4. Lower the powder piston onto the driving system.
5. Then slide the powder feeder so that the next desired powder cylinder is lined up with the delivery system.
6. Repeat step 2–5.
7. Continue for as many different powders and/or powder layers as required.

We created each layer by spreading a thin layer of powder over the surface of a powder bed. The powder bed is supported by a piston that descends upon powder spreading and then prints each layer. More details of 3D printing have been previously described (Wu et al., 1996; Leong et al., 2003; Sachols et al., 2003).

Printed implants were allowed to dry overnight at room temperature, followed by removal of the unbound powder to reveal the final implants. The implants were carefully removed from the plate and transferred into a vacuum oven and allowed to dry for 7 days. We assumed that the migration of polymer and drug during the drying period was minimal.

2.3.2. Conventional compression process

The implant paste was made by adding drug directly as powder or incorporated as an emulsion of polymer solution prior to mixing and drying. These implants, therefore, were manufactured by creating homogeneous mixtures of powdered drugs and excipients. The conventional implants in this study were prepared by compressing homogeneous mixtures of L-PLA and LVFX using a process described by Castro et al. (2003), and Soriano and Evora (2000).

2.4. Microscopic observation of implants

Environmental scanning electron microscopy (ESEM) was used to characterize the structure of the implants before, during and after the drug release assays. The samples were dried and coated under an argon atmosphere with gold–palladium and then examined by ESEM (FEI Quanta 200) at 20 kV.

2.5. Analytical method for measuring LVFX

For the in vitro release test, concentrations of LVFX in each released sample lot were analyzed by measuring absorbance at 292 nm with an UV spectrophotometer (PerkinElmer Lambda 35). The in vitro release medium was composed of PBS 7.4 and 0.9% (w/v) sodium chloride. The standard curve was plotted and linear regression allowed quantification of the samples.

2.6. In vitro release assay

The samples were placed in 20 ml glass test tubes with fresh buffer solution, and maintained in water bath at 37 °C. The release medium was sampled at pre-selected intervals for UV absorbance and replaced with fresh physiological saline.

3. Results and discussion

3.1. Selection of the binder for 3D printing

According to reports on the 3D printing technique from MIT (Wu et al., 1996; Leong et al., 2003; Sachols et al., 2003; Jill et al., 2002), the binder used in 3D printing can be the same material as in the conventional powder compression methods (Cima and Cima, 1996; Monkhouse et al., 2003). The optimal binder selection for 3D printing of implants should be determined before their fabrication.

In this study, L-PLA was used as the polymer phase, which was soluble in acetone. The LVFX was slightly soluble in acetone but soluble in ethanol. The solubility of LVFX in different ratios of ethanol and acetone solutions was determined in order to optimize the balance of high drug concentration and dissolution ability of the polymer binder solution. The mixtures of ethanol and acetone (5:95, 10:90, 20:80, 30:70, 40:60, v/v) shown in Table 2 were investigated. A homogeneous implant was achieved by these binders solutions, which was deposited on a bed of L-PLA.

From Table 2, we determined that a 20:80 mixture of ethanol and acetone was suitable for dissolving the polymer L-PLA, while delivering a high concentration of drug to the implant; therefore, binder solutions with ethanol and acetone at 20:80 were selected for subsequent 3D printing.

Table 2
Binder composition of 3D printing process for implants fabrication

	Binder composition	
A	Acetone	Cannot print
B	Acetone + 5% ethanol	Print; cannot bind
C	Acetone + 10% ethanol	Print and bind; loose
D	Acetone + 20% ethanol	Print; bind; excellent
E	Acetone + 30% ethanol	Print and bind; normal
F	Acetone + 40% ethanol	Print; bind; poor

3.2. Microscopic observation of implants

Implants manufactured by 3D printing are shown in Fig. 3. The surface of the implants appeared smooth and the implants have the external dimension of 6 mm in height and 9 mm in diameter.

The morphology of the implants made using the two processes was compared. The implant made by the conventional compression process had fewer pores while the implant made by 3D printing technique was more porous and uniform. The same uniform predefined structure of implant III with a pore size of below 200 μm is shown in Fig. 4.

The structure of implant III during the release test at 40th day was characterized by ESEM (Fig. 5). The pore size was 200–400 μm, and most remained connected during the period of drug release. This pore size range has been shown as optimal for regenerating bone scaffolds (Leong et al., 2003; Jill et al., 2002). This suggests that the 3D implants we describe here may also have utility as an implant matrix for bone repair. As the drug release study progressed over time, the connected pore size became about 500 μm after 100 days. Follow-up studies in vivo in a rabbit model to measure drug release and bone repair of the implants we describe here are in progress (data not shown).

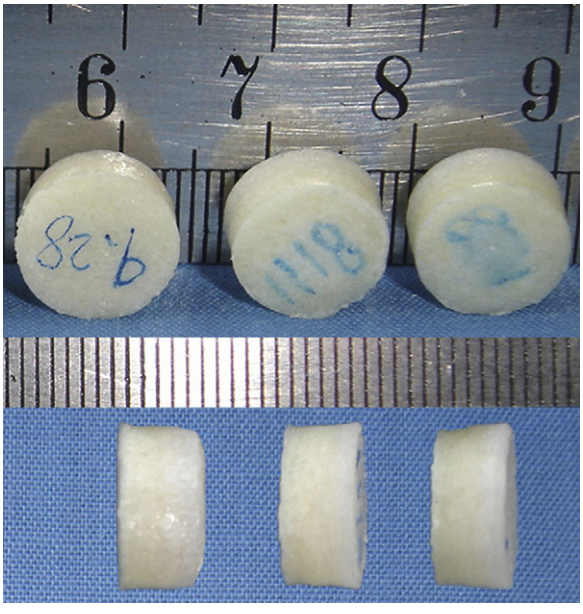

Fig. 3. The typical implants fabricated by 3D printing process. The scale of the ruler is mm.

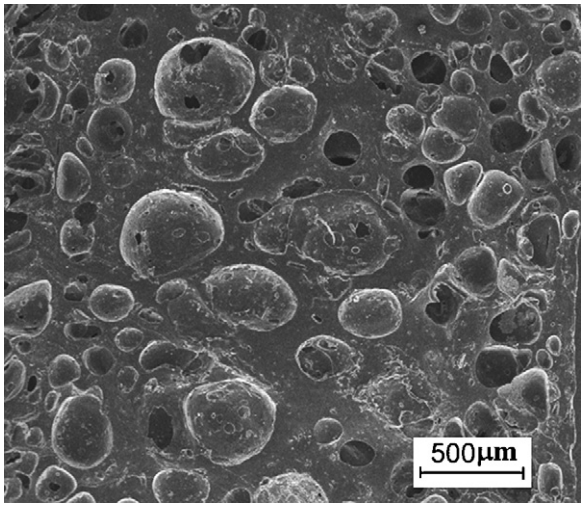

Fig. 4. The cross-section ESEM of implant III made by 3D printing process.

3.3. In vitro measurements

Fig. 6a shows the release of implant I made by the conventional compressing process. The release of implant I reached maximum concentration of 19 μg/ml at the 5th day. After about 15 days, LVFX release was around 6 μg/ml and remained below 4 μg/ml from days 20 to 42. The result of implant I made by 3D printing in Fig. 6b indicated that burst release occurred, following a lag time of 1 day, at the 4th day. The concentration of LVFX release was maintained about 4 μg/ml for 15 days before declining gradually to under 4 μg/ml on day 42.

From the release profiles of Fig. 6a and b, implant I made by both techniques appeared to have similar release patterns. The high burst phase of LVFX release was observed between days 4 and 5. The implant made by conventional compressing can sustain a LVFX concentration above 4 μg/ml longer than the implant made by 3D printing. The release pattern may be rationalized by the built-in release mechanism in the cases of the two implants. Both implants achieved a burst of release at almost the same time since the LVFX release starts mostly at

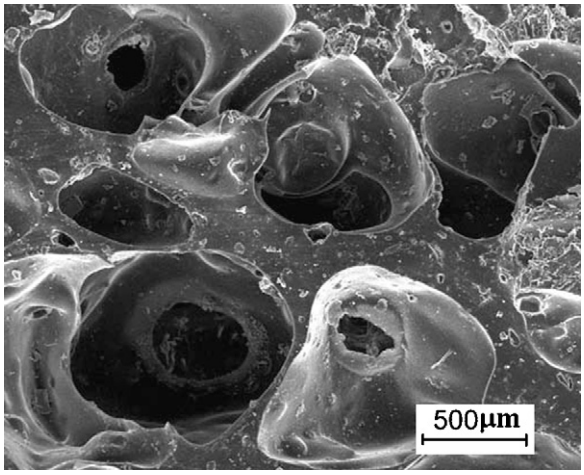

Fig. 5. The cross-section ESEM of implant III after in vitro release for 40 days.

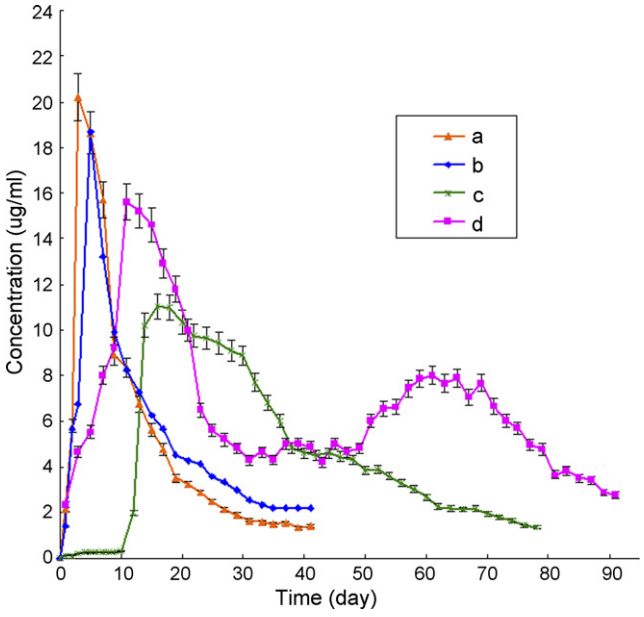

Fig. 6. In vitro release of LVFX from implant I–III, data show mean ± S.D.,($n = 5$). (a) Implant I made by 3D printing process; (b) implant I made by conventional process; (c) implant II made by 3D printing process; (d) implant III made by 3D printing process.

the surface of the implant. From the microscopic observation on implants made by both processes, the implant made by 3D printing displayed a looser or more porous structure than that by the conventional compressing process. This observation suggests that drug release from implants fabricated by 3D printing proceeds by diffusion more readily compared to the conventional compression process, based on the expected patterns of diffusion-mediated drug release reported in the literature (Jill et al., 2002).

The structures of implants made by the conventional fabrication process are relatively simple due to limits in its fabrication technology. The structures of implants fabricated with 3D printing process can be more complex and achieve sophisticated release profiles, as shown by the results from implants II and II.

Fig. 6c and d showed the profiles of implants II and III fabricated by 3D printing process. The LVFX release profile depicted in Fig. 6c indicates that implant II released a higher daily dose of drug overall than implant I, except for the burst release phase. From the 10th to 50th days, implant II achieved a LVFX concentration above 4 μg/ml, with the maximum concentration of 11 μg/ml achieved at 20th day. Implant III was observed to have a distinct bi-modal or pulsed pattern of release, as shown by Fig. 6d. The first phase of the pulsed release of LVFX appeared from the 5th to 25th day, and the highest concentration achieved during this period was 15 μg/ml at the 15th day. A steady state period of 25 days then occurred, with drug release during this time measured at about 5 μg/ml per day. A second pulse of drug release began at 50th day and ended at 80th day, and the highest concentration was 8 μg/ml at the 65th day. The release concentration was below 2 μg/ml at the 95th day in this 100-day study.

Release studies for each of the implant designs were undertaken to gain better insight into the impact of different fabrication processes on drug release over time. The in vitro release profiles in Fig. 6a–d indicated that all the implants continued to liberate LVFX, but at nonlinear kinetics, throughout the 40-days study for implant I, for about 80-days for implant II and for about 90-days for implant III. The release pattern of LVFX from the implants was variable, which suggests that the release was likely controlled by a combination of passive diffusion and erosion of the polymer matrix over time according to the bioerosion-modulated drug release mechanisms (Chein, 1992).

Since the internal, macroscopic architecture of drug implants can be more carefully designed and fabricated using the 3D printing technique, implants could be created with many regions, each with different materials and architectures, as shown in Fig. 2 II and III. The release profiles of implant II and III shown in Fig. 6c and d met the designed criteria of the predefined microstructure fabricated by 3D printing. The sophisticated release profiles of such implants may suggest that 3D printing techniques have the potential to allow fabrication of implants with more complex drug release profiles than are possible with conventional manufacturing techniques. The former may find specific therapeutic applications where bi-modal or other patterns of drug exposure are highly desirable, but not achievable with conventional methods routinely used today.

4. Conclusions

Using a novel 3D printing technique, we successfully fabricated drug implants containing LVFX with predefined microstructures that exhibited complex release profiles not achievable with conventional fabrication methods. The optimal binder in our process was 20:80 (v/v) ethanol and acetone. Three implants demonstrating proportional release were developed using 3D printing versus conventional molding. The microscopic morphologies and the in vitro release of the implants were investigated using ESEM and UV spectrophotometric absorption at 292 nm to evaluate the performance of both types of implant devices.

In comparison with the implants fabricated by the conventional technology, the implants we prepared by 3D printing process achieved a more sophisticated drug release profile; namely a distinct bi-modal, or pulsed release profile from a single implant. Over the course of 100 days of monitoring drug release in vitro, one pulse of release appeared from the 5th to 25th day, and another pulse began at the 50th day and ended at 80th day, with a lag time of 25 days between the two pulses, wherein a steady state of release was observed at about 5 μg/ml of LVFX.

We show that such 3D implants can display complex drug release patterns compared to conventionally fabricated drug implants. Our study provides support that 3D printing methodologies that deploy inkjet techniques have promising potential for manufacturing sophisticated drug implants with bi-modal release profiles that could have new therapeutic applications.

Acknowledgement

We would like to thank the following individuals for their assistance in this project: Tang Hangu, Yu Denguang, and Wang Zhiqing.

References

Achim, G., 1997. Bioerodible implants with programmable drug release. J. Control Release 44, 271–281.

Alekha, K.D., Greggrey, C.C., 1998. Therapeutic applications of implantable drug delivery systems. J. Pharmacol. Toxicol. Methods 40, 1–12.

Castro, C., Sanchez, E., Delgado, A., Soriano, I., Nunez, P., Baro, M., Perea, Evora, C., 2003. Ciprofloxacin implants for bone infection in vitro-in vivo characterization. J. Control Release 93, 341–354.

Chein, Y.W., 1992. Novel Drug Delivery Systems, second ed. Marcel Dekker Inc., New York, NY, pp. 445–460.

Cima, L.G., Cima, M.J., 1996. Preparation of medical devices by solid free-form fabrication methods. U.S. patent 5,490,962, 13, February.

Gabriel, T.M., David, G., Scott, J., 2002. Mechanical and in vivo performance of hydroxyapatite implants with controlled architectures. Biomaterials 23, 1283–1293.

Huang, W.D., Sun, W.Q., Zheng, Q.X., Guo, X.D., Yu, D.G., Liu, W., Xu, H.B., Yang, X.L., 2005. Design and fabrication of drug delivery devices with complex architectures based on three-dimensional printing technique. J. Wuhan Univ. Technol.-Mater. Sci. Edit. 20, 80–82.

Jill, K.S., Susan, L.R., Robert, P., Scott, C.B., Donald, C.M., Matt, C., Linda, G.G., Lee, K.L., Anthony, R., 2002. A three-dimensional osteochondral composite scaffold forarticular cartilage repair. Biomaterials 23, 4739–4751.

Katsta, W.E., Palazzolo, R.D., Rowe, C.W., Giritlioglu, B., Teung, P., 2000. Oral dosage forms fabricated by three dimensional printing. J. Control Release 66, 1–9.

Kim, S.S., Utsunomiya, H., Koski, J.A., Wu, B.M., Cima, M.J., Sohn, J., Mukai, K., Griffith, L.G., Vacanti, J.P., 1998. Survival and function of hepatocytes on a novel three-dimensional synthetic biodegradable polymer scoffold with intrinsic network of channels. Ann. Surg. 228, 8–13.

Lam, C.X.F., Mo, X.M., Teoh, S.H., Hutmacher, D.W., 2002. Scoffold development using 3D printing with a starch-based polymer. Mater. Sci. Eng. C 20, 49–56.

Leong, K.F., Cheah, C.M., Chua, C.K., 2003. Solid freeform fabrication of three-dimensional scaffolds for engineering replacement tissues and organs. Biomaterials 24, 2363–2378.

Monkhouse, D., Yoo, J., Sherwood, J., Cima, M.J., Bornancini, E., 2003. Dosage forms exhibiting multi-phastic release kinetics and methods of manufacture thereof. U.S. patent 6,514,518 B2, 4 February.

Park, A., Wu, B., Griffith, L.G., 1998. Integration of surface modification and 3D fabrication techniques to prepare patterned poly (L-lactide) sbustrate allowing regionally selective cell adhesion. J. Biamater. Sci.-Polym. E 9, 89–110.

Rowe, C.W., Katsta, W.E., Polazzolo, R.D., Giritlioglu, B., Teung, P., Cima, M.J., 2000. Multimechanism oral dosage forms fabricated by three dimensional printing. J. Control Release 66, 11–17.

Sachols, E., Reis, N., Ainsley, C., Derby, B., Czernuszka, J.T., 2003. Novel collagen scaffolds with prefined internal morphology made by solid freeform fabrication. Biomaterials 24, 1487–1497.

Sarah, L.T., Tejal, A.D., 2003. Microfabricated drug delivery systems: from particles to pores. Adv. Drug Deliv. Rev. 55, 315–328.

Soriano, I., Evora, C., 2000. Formulation of calcium phosphates/poly (D,L-lactide) blends containing gentamicin for bone implantation. J. Control Release 68, 121–234.

Wu, B.M., Borland, S.W., Giordano, R.A., Cima, L.G., Sachs, E.M., Cima, M.J., 1996. Solid free-form fabrication of drug delivery devicess. J. Control. Release 40, 77–87.

Zeltinger, J., Sheerwood, J.K., Graham, D.M., Mueller, R., Griffith, L.G., 2001. Effects of pore size and void fraction on celluar adhesion, proliferation, and matrix deposition. Tisse Eng. 7, 557–572.

Zheng, Q.X., Guo, X.D., Du, J.Y., 2002. Biodegradation of absorbable HA/dl-PLA composites in different environment. J. Wuhan Univ. Technol.-Mater. Sci. Edit. 17, 24–29.

Zhou, T.H., Lewis, H., Foster, R.E., Schwendeman, S.P., 1998. Development of a multiple-drug delivery implant for intraocular management of proliferative vitreoretinopathy. J. Control Release 55, 281–295.